

Tunneling current through a possible all-perovskite oxide p - n junction

Yukio Watanabe

Kyushu Institute of Technology, Kitakyushu 804, Japan

(Received 27 October 1997)

An anomalous increase of electric conduction with decreasing temperature was found in the current through $\text{Pb}(\text{Ti,Zr})\text{O}_3$ ferroelectric/ SrTiO_3 epitaxial heterostructures. Comparison with current-voltage characteristics of other ferroelectric epitaxial heterostructures and the analysis using the band diagram indicate that the current is tunneling through the p - n junction formed by $\text{Pb}(\text{Ti,Zr})\text{O}_3$ and SrTiO_3 , which have been regarded as insulators so far. [S0163-1829(98)51910-8]

Tunneling current was predicted by Wilson, Frenkel, and Joffe 65 years ago.¹ It was discovered in a narrow Ge p - n junction (p : hole carrier, n : electron carrier) by Esaki 40 years ago,² which encouraged the discovery of superconducting tunneling and the Josephson device. Subsequently, tunneling current in various structures such as semiconductor heterojunctions, metal/insulator/semiconductor, has been reported.^{3,4} However, no tunneling current through an oxide p - n junction has been reported so far.

Conventionally, a ferroelectric is treated as an insulator. However, a typical ferroelectric like BaTiO_3 and PbTiO_3 has a band gap of 3 eV, and recent studies of the leakage current through it indicate metal/semiconductor properties at the metal/ferroelectric interface.⁵ The present paper reports more drastic evidence for the semiconductivity of ferroelectric. Namely, a phenomenon reported here suggests two properties of ferroelectric: evidence of a p - n junction formation by ferroelectric perovskites, which is possible in principle, and the observation of a tunneling current through *all-oxide semiconductor* p - n junction. The p - n junction formation in ferroelectric heterostructures opens a possibility of developing a class of semiconductor heterostructures and also ferroelectrically tunable p - n junctions, in addition to a ferroelectric field effect transistor.⁶ Additionally, semiconductivity of ferroelectric has an important implication on the mechanism for suppressing the finite-size effect of ferroelectricity.⁷

The principal result of the present paper is an anomalous increase of the reverse-bias current with decreasing temperature (T) in Fig. 1(a). We attribute this to the tunneling through the p - n junction of $\text{PbZr}_{0.5}\text{Ti}_{0.5}\text{O}_3$ /Nb-doped SrTiO_3 , as discussed below.

Five types of heterostructures were grown for the current dc-voltage (IV) measurement: PZT/STON, PZT/LCO, PLZT/STON, PLZT/LCO, and PLZT10/LCO, where LCO, STON, PZT, PLZT, and PLZT10 represents $\text{La}_{1.99}\text{Sr}_{0.01}\text{CuO}_4$, SrTiO_3 :Nb 0.5 wt %, $\text{PbZr}_{0.5}\text{Ti}_{0.5}\text{O}_3$, $\text{Pb}_{0.95}\text{La}_{0.05}\text{Zr}_{0.2}\text{Ti}_{0.8}\text{O}_3$ and $\text{Pb}_{0.9}\text{La}_{0.1}\text{Zr}_{0.2}\text{Ti}_{0.8}\text{O}_3$, respectively. LCO films were grown on SrTiO_3 (STO), and STON was the substrate. The thickness of all Pb-ferroelectric layers (except for PLZT10) and LCO was approximately 200 nm and 100 nm, respectively.

PZT films are reported to have an acceptor density N_A of 10^{17} – 10^{18} cm^{-3} , and its Fermi level is close to the valence band edge.⁸ The effect of La doping to PZT is established

experimentally to compensate the hole carriers and increase the resistivity.⁹ LCO films and STON substrates are estimated to have an acceptor density of 1×10^{19} cm^{-3} and a donor density N_D of 5×10^{19} cm^{-3} , respectively.

The x-ray $\theta/2\theta$ scan and the x-ray pole figure diffractometry showed three-dimensional alignment of the layers and the substrates in the heterostructures. The lattice mismatch between a axes of PZT and STON is 2.8%, and PZT was

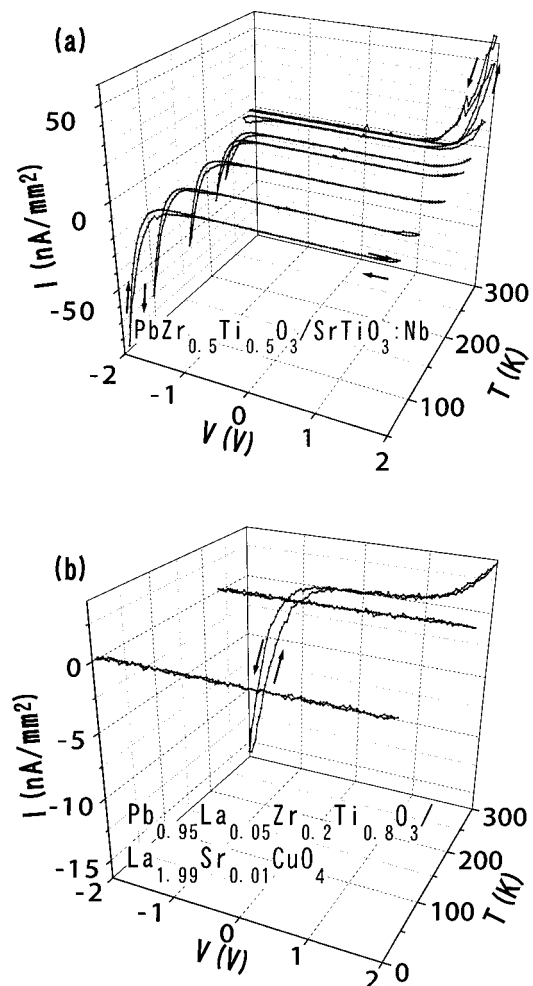


FIG. 1. Temperature (T) dependence of IV hysteresses of PZT/STON (a) and PZT/LCO (b). The arrows indicates the direction of scan.

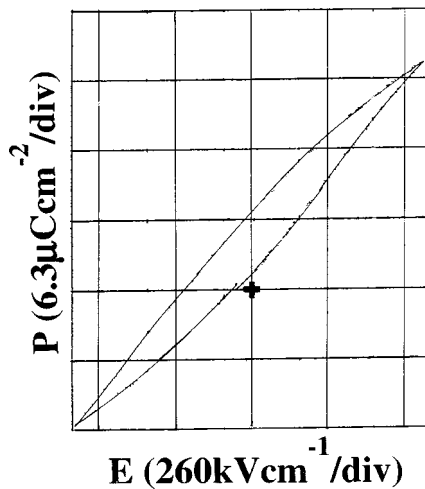


FIG. 2. Polarization (P)-voltage (E) hysteresis of PZT/STON at 1 kHz at RT. No resistance compensation was performed. The symbol + indicates the position for $E=P=0$.

mostly [001] oriented with a mixture of [100] orientation. No secondary phases were detected by the depth profile using secondary ion mass spectroscopy, auger electron spectroscopy and x-ray diffractometry. The top and bottom electrodes are Au films (1 nm^2) on the ferroelectric and Ag, Al, or In films ($10\text{--}50 \text{ nm}^2$) on STON and LCO, respectively. Figure 2 shows an example of the polarization hysteresis loop of PZT/STON. One cycle of IV curve was measured approximately in 7 min, with the voltage polarity being defined at the top metal electrode. Between 4 K and RT (room temperature) the resistance of STON substrate and LCO films alone were lower by over 10^4 than the total resistance of the diode.¹⁰

In the T dependence of IV curves of Au/PZT/STON in Fig. 1(a), a diodelike current is evident at positive bias exhibiting conductivity enhancement above 270 K and decreases with reducing T . On the other hand, the current grows at negative bias with reducing T . A pair of IV curves near 300 K before and after the IV measurements at low T are almost identical, indicating no irreversible change during the measurement. This phenomenon was observed reproducibly and consistently in other PZT/STON samples and PLZT/STON.

On the contrary, no anomalous behavior was observed in Au/PLZT/LCO and Au/PLZT10/LCO. In Figs. 1(b) and 3, diodelike current was observed at negative bias exhibiting conductivity enhancement at 290 K and decreased with reducing T . Diodelike current was suppressed at 84 K for the bias scan amplitude of $\pm 3 \text{ V}$. However, IV characteristics similar to those at 290 K reemerged at 84 K, by increasing the bias scan amplitude up to $\pm 5 \text{ V}$ (Fig. 3). These observations and the resistance of LCO films measured separately eliminate the resistance increase of the bulk conduction in LCO and of the contact at LCO surface as an origin of the disappearance of current at low T .

The other sources of the resistance are the conduction through PZT, the contact resistance of Au/PZT and the junction resistance of PZT/STON or PZT/LCO. Therefore, the difference of IV curves in Figs. 1(a) and 1(b) exists in the difference between the PZT/STON and PZT/LCO junctions.

Indeed, the polarity of the forward bias in the present

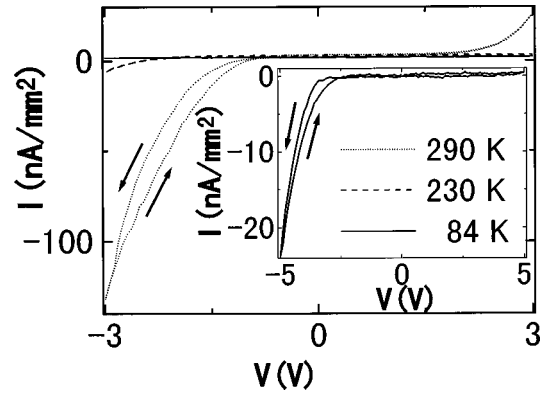


FIG. 3. T dependence of IV hysteresis of PLZT10/LCO [(\cdots) 290 K, ($---$) 230 K, ($—$) 84 K]. The inset shows an IV hysteresis at 84 K with the maximum voltage scale of $\pm 5 \text{ V}$.

heterostructures is always positive for STON bottom electrode and negative for LCO bottom electrode at RT. This polarity dependence was confirmed in several other combinations of ferroelectric and the perovskite conductors.¹¹ IV is determined by the most resistive part in the current path.

The band diagram based on the work function difference like Fig. 4(a) was able to explain consistently IV curves of various heterostructures above RT.¹¹ For example, we assume a p - n junction at PZT/STON interface. All the polarity dependences observed so far are explained by noting the magnitude of the band bending, i.e., the built-in potential at the ferroelectric surfaces. In PZT/STON, the reverse-bias current is determined by a p - n PZT/STON junction, because its built-in potential exceeds that of the Au/PZT contact [Fig.

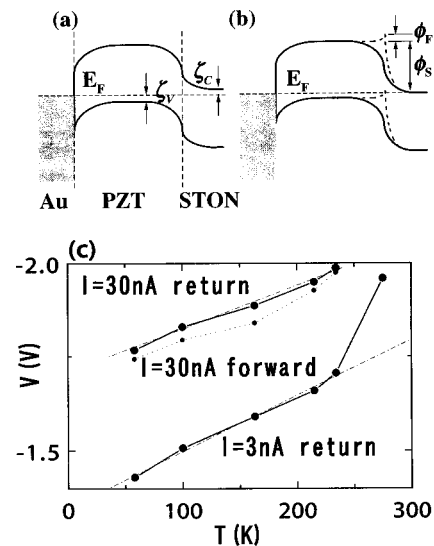


FIG. 4. Band diagrams of Au/PZT/STON at RT (a) and at low T (b) and the T dependence of the voltage for reaching the current densities of 3 nA/mm^2 and 30 nA/mm^2 (c). The difference between the band diagrams (solid lines) at low T and at RT is the reduction of ξ_V and ξ_C at low T . The dashed lines in (b) show a band diagram for a stable P_s ($\approx -40 \mu\text{C cm}^{-2}$) that yields $\phi_F \ll \phi_S \approx 3 \text{ V}$ according to the procedure described in Ref. 7, and the total depletion width is calculated to be 5 nm for $\epsilon=5$. In (c), for a current of 30 nA/mm^2 , voltages at both increasing ($-\cdots-\cdots-$) and decreasing ($-\bullet-\bullet-$) magnitudes are plotted. The lines $-\cdots-\cdots-$ are the best fittings to the data.

4(a)]. Similarly, the built-in potential at PZT/LCO p - p junction is less than that at Au/PZT. Therefore, the reverse bias of Au/PZT/LCO corresponds to the reverse-bias polarity of the Au/PZT.¹²

If the tunneling current is not dominant in the total current, the resistances at these interfaces mainly determine the overall resistance and increase as T decreases. Furthermore, the quantum paraelectricity below 40 K induces the large increase of the dielectric constant ϵ of STON at low T ,¹³ which widens the depletion layer at PZT/STON junction with decreasing T . This enhances the resistance at PZT/STON.

The tunneling current through Au/PZT becomes important at low T . The ratio of the tunneling current to the thermionic emission current through metal/semiconductor contact increases with reducing T and increasing doping. However, the total current does not increase at least with decreasing T .¹⁴ The change of the depletion layer width through the change of ϵ of PZT is negligible, due to the high Curie temperature of PZT.

Therefore, the only cause of the increasing current density with decreasing T is searched at the PZT/STON interface. One source is a possible change of the built-in potential induced by the phase transition of a tetragonal PZT into a rhombohedral PZT, which is observed in bulk material near 300 K. However, the increase of the reverse current continued, at least, to 60 K. Furthermore, the T dependence of the current in PLZT/STON was similar to PZT/STON, while no phase transition of PLZT is expected near 300 K.

The band diagram of PZT/STON at RT at zero bias in Fig. 4(a) suggests a possibility of the tunneling current at reverse bias. Even for $\epsilon=5$ of STON and PZT,¹⁵ the depletion layer width is estimated to be approximately 30 nm ($N_A=10^{18}$ cm⁻³)~100 nm ($N_A=10^{17}$ cm⁻³) and is very wide, as compared with those of ordinary tunnel junctions. However, the various experiments and analyses discussed above and the below suggest that tunneling is the most plausible conduction mechanism for Fig. 1(a). First, the replot of Fig. 1(a), i.e., Fig. 5, demonstrates that the Fowler-Nordheim-type tunneling fits the results satisfactorily for $V < 0$.

For tunneling through a p - n junction, the reduction of the doping density, i.e., the increase of the band offset suppresses tunneling. The La substitution into Pb of PZT (PLZT) reduces the hole concentration as mentioned above, which implies the increase of the band offset ξ_V of PLZT in a rigid-band model. Indeed, the current at the reverse bias was drastically reduced in all T , while it still showed an increasing reverse current with decreasing T (Fig. 6). This result is difficult to explain by direct tunneling and other conduction mechanisms.

For the tunneling current to grow with decreasing T , a certain effect must overcome the increase of the depletion layer width or other sources of the resistance increase. Figure 4(b) shows the answer. The band offset ξ_V is given by $k_B T \ln N_V/N_A$, where k_B : Boltzmann constant, $N_V \propto T^{3/2}$: effective density state of the valence band. Therefore, ξ_V is approximately proportional to T between 58 and 300 K. The tunneling probability is mainly determined by the relative position of the top of the PZT valence band and the bottom of the STON conduction band. Therefore, the bias voltage

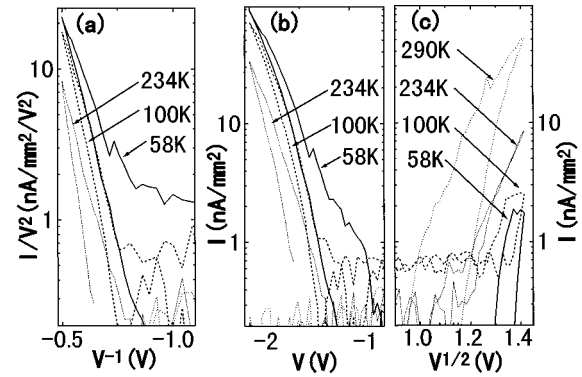


FIG. 5. Replot of a part of Fig. 1(a). For $V < 0$, Fowler-Nordheim tunneling plots of IV data (a) are slightly better than $\log I$ plots (b). For $V > 0$, Schottky plots were the most suitable among the various plots such as Poole-Frenkel, space charge limited, Fowler-Nordheim tunneling, $\log I$, and others.

dependence of tunneling current is a function of $V - \xi_V - \xi_C$ ($\xi_C = k_B T \ln N_C/N_D$, where $N_C \sim N_V$ is the effective density of states of the conduction band). This implies that the voltage for reaching a given density varies with T to satisfy $V - \xi_V - \xi_C = \text{constant} \approx V - ak_B T$ ($k_B T$ is measured in volts, e.g., $k_B T = 26$ mV for $T = 300$ K). Figure 4(c) shows the voltage for reaching 3 nA/mm² and 30 nA/mm² and confirms the linear dependence on T .

Assuming tentatively $N_V = 10^{21}$ cm⁻³ for PZT and STON, we have $\xi_V = 7k_B T - 9k_B T$ and $\xi_C = 3k_B T$ and, therefore, $a = 10$ –12. The fitting to the data in Fig. 4(c) yields $a = 14.2$ for 3 nA/mm² and $a = 11.6$ for 30 nA/mm². The agreement is satisfactory.¹⁶

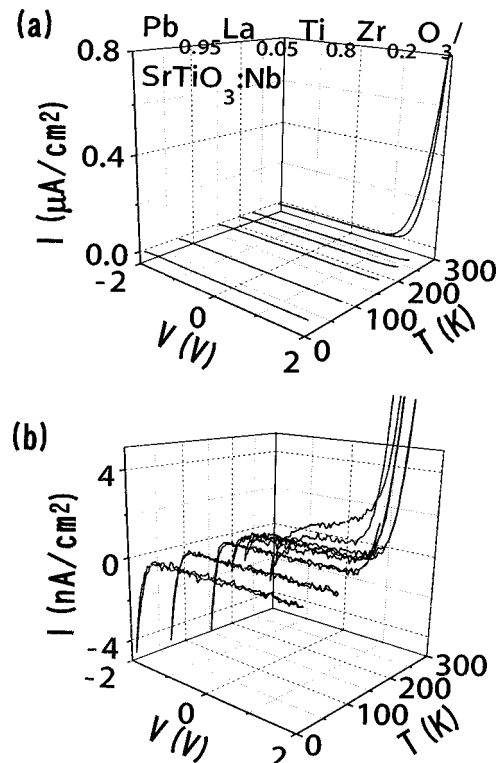


FIG. 6. Temperature dependence of IV hysteresis of PLZT/STON (a) and its blowup view (b). The PLZT film has the same thickness as the film PZT in Fig. 1(a).

These analyses are valid also when the spontaneous polarization P_S and the charged traps modify the electronic state near the interface. As shown by dashed curves in Fig. 4(b), a finite P_S can possibly reduce the depletion layer width in PZT (Ref. 7) which seemed too thick for tunneling through the p - n junction. If this explanation is correct, the tunneling current is controllable by the switching of P_S .

In conclusion, an anomalous increase of the current density with decreasing T was found in Au/PZT/STON, which was not observed in Au/PZT/LCO. This difference was attributed to the PZT/STON p - n junction and the PZT/LCO p - p junction. The examination of the tunneling through Au/PZT, IV characteristics, T dependence indicates the anomalous

current is due to the tunneling through the PZT/STON p - n junction that is possibly influenced by P_S . The analyses suggest that increase of the doping density can enhance the tunneling current and realize the negative resistance. Furthermore, the tunnel diode can be tunable by P_S , which is in progress. The p - n junction formation by ferroelectric perovskites can be extended to a p - n junction formation by other perovskites like manganese perovskite oxides and high- T_c superconductors.

This work was performed under the support of Grant-in-aid for Scientific Research from the Ministry of Education, Science, Sports and the Sumitomo Foundation. Y.W. acknowledges useful discussions with Professor S. Uchida.

-
- ¹A. H. Wilson, Proc. R. Soc. London, Ser. A **136**, 487 (1932); J. Frenkel and A. Joffe, Phys. Z. Sowjetunion **1**, 60 (1932); L. Nordheim, Z. Phys. **75**, 434 (1932).
- ²L. Esaki, Phys. Rev. **109**, 603 (1958).
- ³J. V. Morgan and E. O. Kane, Phys. Rev. Lett. **3**, 466 (1959); N. Holonyak, Jr., J. Appl. Phys. **31**, 130 (1960); L. L. Chang, P. J. Stiles, and L. Esaki, *ibid.* **38**, 4440 (1967).
- ⁴J. C. Mariani, IBM J. Res. Dev. **4**, 280 (1960).
- ⁵For example, P. C. Joshi and S. B. Krupanidhi, J. Appl. Phys. **73**, 7627 (1993); G. W. Dietz, W. Antpohler, M. Klee, and R. Waser, *ibid.* **78**, 6113 (1995).
- ⁶S. Mathews, R. Ramesh, T. Vankatesan, and J. Benedetto, Science **276**, 238 (1997); Y. Watanabe, M. Tanamura, and Y. Matsumoto, Jpn. J. Appl. Phys., Part 1 **35**, 1564 (1996); Y. Watanabe, Appl. Phys. Lett. **66**, 1770 (1995).
- ⁷Y. Watanabe, Phys. Rev. B **57**, 789 (1998).
- ⁸P. F. Baude, C. Ye, and D. L. Polla, Appl. Phys. Lett. **64**, 2670 (1994); G. R. Fox and S. B. Krupanidhi, J. Appl. Phys. **74**, 1949 (1993); C. Sudhama *et al.*, *ibid.* **75**, 1014 (1994).
- ⁹This is simply understood as the substitution of Pb^{2+} with La^{3+} , which makes one electron per La^{3+} , if O, Ti, and Zr concentration is unchanged. Additionally, La substitution to PZT/LCO does not change qualitative features of the temperature dependence of the IV . Therefore, in the caption of Fig. 1 and one paragraph in the text, the heterostructure for Fig. 1(b) is written as PZT/LCO, although it should be written as PLZT/LCO. This is to simplify the discussion that uses the comparison of Figs. 1(a) and 1(b). For a transparent discussion, the comparison of Figs. 6(b) and 1(b) is appropriate, although this does not change the related discussions and the conclusion at all.
- ¹⁰The contact resistance at STON/metal (In, Al) was lower by a factor of 10^3 than the total resistance of the diode.
- ¹¹Y. Watanabe, Appl. Phys. Lett. **66**, 28 (1995); Y. Watanabe, D. Sawamura, N. Toyama, and M. Okano, Proceedings of the 9th International Meeting on Ferroelectrics [J. Korean Phys. Soc. (to be published)].
- ¹²We have also confirmed that the density of the current through metal/PLZT/STON (p - n junction) and $BaTiO_3$ /LCO (n - p junction) was insensitive to the metal electrode material (Al, Au, Pt), while that through $BaTiO_3$ /STON (n - n junction) and PLZT/STON (p - p junction) was very sensitive to the material.
- ¹³K. A. Nüller and H. Burkard, Phys. Rev. B **19**, 3593 (1979).
- ¹⁴C. Y. Chang and S. M. Sze, Solid-State Electron. **13**, 727 (1970).
- ¹⁵Many experimental results for the current through metal/ferroelectric junctions are inexplicable if we use a low-frequency ϵ of the ferroelectric, and an optical ϵ is frequently employed. This is probably related to the fact that optical ϵ is due to deformation of electron cloud as in Si, while low-frequency ϵ is due to ion motion specific to ferroelectric.
- ¹⁶If the current at $V < 0$ is tunneling directly from the metal through PZT to STON, its T dependence is inexplicable for plausible values of N_D and N_V of STON. Furthermore, the thickness of PZT is too thick for a conventional tunneling. Similarly, if the low-frequency ϵ of PZT and STON (> 200) is used, the depletion layer width exceeds 200 nm, for which a conventional tunneling is also difficult unless we use the band diagram for $P_S \neq 0$ [Fig. 4(b)]. If use of an optical ϵ is appropriate, the T dependence of ϵ discussed in the text is unnecessary. The diode corresponding to Fig. 4(b) exhibits no tunneling at forward bias and no negative resistance (backward diode) but may when it is more heavily doped.